

**Chaotic route to classical thermalization: A real-space analysis**Yue Liu and Dahai He <sup>\*</sup>*Department of Physics and Jiujiang Research Institute, Xiamen University, Xiamen 361005, Fujian, China*

(Received 7 February 2024; revised 16 April 2024; accepted 23 May 2024; published 6 June 2024)

Most of the previous studies on classical thermalization focus on the wave-vector space, encountering limitations when extended beyond quasi-integrable regions. In this study, we propose a scheme to study the thermalization of the classical Hamiltonian chain of interacting oscillators in real space by developing a thermalization indicator proposed by Parisi [*Europhys. Lett.* **40**, 357 (1997)], which approaches zero in the thermal state. Upon reaching the steady state characterized by the generalized Gibbs ensemble for a harmonic chain, a quench protocol is implemented to change the Hamiltonian to a nonintegrable form instantaneously, thereby preparing nonequilibrium initial states. This approach enables investigations of thermalization in real space, particularly valuable for exploring regions beyond quasi-integrability. For the FPUT- $\beta$  lattice, we observe that the thermalization time as a function of the nonintegrable strength follows a  $-2$  scaling law in the quasi-integrable region and  $-1/4$  in the strongly integrable region. Moreover, numerical results reveal the thermalization time is proportional to the Lyapunov time, which bridges microscopic chaotic dynamics and the macroscopic thermalization process.

DOI: [10.1103/PhysRevE.109.064115](https://doi.org/10.1103/PhysRevE.109.064115)**I. INTRODUCTION**

Whether and how a given nonequilibrium initial state evolves to the desired thermal state of a Hamiltonian system is the central question of nonequilibrium statistical physics, receiving significant research interests in decades [1–7]. Thermalization requires the average of the observables for infinite time to match with the average in phase space. The mode energy in wave-vector space was chosen as the observable to study ergodization by Fermi, Pasta, Ulam, and Tsingou (FPUT) for the first computer experiment [8], of which the main aim was to observe the thermalization in a nonlinear isolated system. Surprisingly, they found that systems with small nonlinearity seem incapable of relaxing to the equilibrium state, but exhibit a complicated quasiperiodic behavior, which keeps a memory of the initial conditions. The phenomenon is called the FPUT paradox and suggests that the ergodicity fails in the system. The pursuit of this unexpected result triggered the observation of solitons [9] and the development of Hamiltonian chaos [10]. From today's point of view, the quasiperiodic behavior corresponds to the metastable state according to both analytical arguments [11] and numerical simulations [12–14], which indicates that systems with small nonlinearity can approach to equilibrium in longer timescales. In terms of the wave-turbulence theory, it has been found that the thermalization time as the function of the nonintegrable strength exhibits scaling behaviors with exponent  $-2$  in the quasi-integrable region in the thermodynamic limit [7, 15–18].

The Hamiltonian systems that can relax to a thermodynamic equilibrium state from a nonequilibrium initial state generally show chaotic features, which suggests macroscopic

relaxation phenomena can be traced back to microscopic dynamics. In the quasi-integrable region, it has been shown that the thermalization time is proportional to the Lyapunov time (the inverse of the maximum Lyapunov exponent) [19]. However, beyond the quasi-integrable region, the relationship between the two timescales is unclear. It lies in the problem that the mode energy in the wave-vector space is ill-defined beyond the quasi-integrable region. A natural alternative approach is to study thermalization in real space. Some methods have been proposed to describe the behavior of thermalization in real space. Parisi has employed the nearest correlation in real space to investigate the relaxation time by its logarithmic derivative of time [20]. By this method, one can observe that the thermalization time shows the exponential stretching behavior as a function of anharmonicity. Through studying the fluctuation of observable, the ergodization time can be defined, which shows qualitatively different behaviors to the Lyapunov time [21, 22]. Meanwhile, a study of thermalization of the local observable [23] demonstrates that the scaling behavior of the equilibration time depends on the initial condition, showing the lack of universality. Despite significant strides made in understanding the issue, how to appropriately define the thermalization time in real space is still under debate.

In this paper, we employ an observable  $\Delta(t)$  introduced in Ref. [20] as a real-space indicator of thermalization. We propose a scheme for determining the thermalization time based on this indicator's evolution. The values of  $\Delta$  for the integrable harmonic lattice should be determined by the generalized Gibbs ensemble (GGE), which is a nonzero value generally. One can prepare nonequilibrium initial conditions by quenching the harmonic system to a nonintegrable model and obtain the thermalization time by investigating  $\Delta(t)$ . We apply the scheme to the FPUT- $\beta$  lattice and find that the

<sup>\*</sup>dhe@xmu.edu.cn

thermalization time displays a double scaling behavior with respect to the nonintegrable strength. Specifically, the scaling behavior in the quasi-integrable region agrees with the wave-turbulence theory, while it transitions to another scaling exponent in the strongly nonintegrable region. Moreover, our numerical results show that the thermalization time is proportional to the Lyapunov time in a wide range of nonintegrable strength. Our results not only link the chaotic dynamics and relaxation process but also provide a scheme to study classical thermalization.

The paper is organized as follows. In Sec. II, we introduce the model and methods used in this study, in particular the indicator  $\Delta$ , GGE and the quench protocol. In Sec. III, we apply the quench protocol to the FPUT- $\beta$  system to study the thermalization time in a wide range of nonintegrable strengths. Finally, we summarize our main results and give a discussion in Sec. IV.

## II. MODEL AND METHODS

For isolated one-dimensional lattices described by Hamiltonian

$$H = \sum_n \frac{p_n^2}{2m} + V(\delta q_n) + U(q_n), \quad (1)$$

Parisi proposed an indicator for thermalization [20]

$$\Delta = \frac{\langle \sum_n p_n p_{n+1} \rangle}{\langle \sum_n p_n^2 \rangle}. \quad (2)$$

Here,  $p_n$  and  $q_n$  denote the instantaneous momentum and the displacement from the equilibrium position of  $n$ th oscillator, and  $\delta q_n = q_n - q_{n-1}$ . The nearest-neighbor interaction and onsite potential are represented by  $V(\delta q)$  and  $U(q)$ , respectively. The average  $\langle \dots \rangle$  represents the time average. In the following discussions, we set the mass  $m$  and the Boltzmann's constant  $k_B = 1$  as the unit, i.e.,  $m = 1$  and  $k_B = 1$  for brevity. The indicator  $\Delta$  goes to zero in the thermal state for bounded potential, demonstrating that it is appropriate as an indicator of thermalization [24].

### A. Generalized Gibbs ensemble (GGE)

For the integrable harmonic lattice with  $V(x) = x^2/2$  and  $U(x) = 0$ , the indicator  $\Delta$  is not expected to relax to 0. Instead, the expectation value of the observable for integrable systems is predicted by GGE [25–27], of which the probability density function is given by

$$\rho^{\text{GGE}} = \frac{1}{Z^{\text{GGE}}} \exp\left(-\sum_k \chi_k I_k\right). \quad (3)$$

Here  $\{I_k\}$  is a set of  $N$  nontrivial conserved quantities. The validity of GGE has been demonstrated in a variety of one-dimensional models, such as the transverse field Ising model [28,29], hard-core anyons [30], quantum field theories [31], and spin-1/2 XXZ chains [32]. The corresponding partition function of GGE reads

$$Z^{\text{GGE}} = \int \exp\left(-\sum_k \chi_k I_k\right) d\Gamma, \quad (4)$$

where  $\Gamma \equiv (\mathbf{q}, \mathbf{p}) = (q_1, q_2, \dots, q_N, p_1, p_2, \dots, p_N)$  denotes a point in phase space. The expectation value of the observable  $A$  is given by  $\langle A \rangle^{\text{GGE}} = \int A \rho^{\text{GGE}} d\Gamma$ . The set of Lagrange multipliers  $\{\chi_k\}$  are determined by each conserved quantity in the initial state

$$\langle I_k \rangle = I_k(t=0) = \int I_k \rho^{\text{GGE}} d\Gamma. \quad (5)$$

In contrast to the Gibbs ensemble, the expectation values of observables depend on the initial state. For the harmonic lattice, the conserved quantities  $I_k$  for GGE is the mode energy  $E_k$  because of the absence of phonon-phonon interaction, namely,

$$I_k = E_k = \frac{1}{2} P_k^2 + \frac{1}{2} \omega_k^2 Q_k, \quad (6)$$

where  $\omega_k$ ,  $Q_k$ , and  $P_k$  are the frequency, canonical coordinate, and canonical momentum of the  $k$ th mode, respectively. The canonical coordinate and the canonical momentum can be evaluated by the canonical transformation  $Q_k = \sum_{n=1}^N q_n e_k^n$  and  $P_k = \sum_{n=1}^N p_n e_k^n$ , where  $e_k^n$  represents the  $n$ th component of eigenvector of the  $k$ th mode. The partition function of GGE for harmonic systems can be given by

$$Z^{\text{GGE}} = \prod_k \frac{2\pi}{\chi_k \omega_k}. \quad (7)$$

Thus, one can obtain the Lagrange multipliers

$$\chi_k = \frac{1}{E_k}, \quad (8)$$

which suggests that the expectation values of the observable rely on the mode energy, such as  $\langle P_k^2 \rangle = E_k$ . Interestingly, based on GGE, the temperature defined by  $T = \sum_n \langle p_n^2 \rangle / N$  in harmonic systems is equal to the energy density, namely,  $T = \varepsilon'$ , which is independent of the initial state and consistent with the prediction of the Gibbs state. Here, we use the Parseval's theorem  $\sum_n \langle p_n^2 \rangle = \sum_k \langle P_k^2 \rangle$ . This result suggests that the relaxation behaviors of temperature can not distinguish integrable and nonintegrable systems. Moreover, the numerator of Eq. (2) can be written as

$$\sum_n \langle p_n p_{n+1} \rangle = \sum_k \langle P_k^2 \rangle \cos\left(\frac{\pi k}{N+1}\right). \quad (9)$$

Then, the indicator  $\Delta$  for the harmonic system can be obtained

$$\Delta = \frac{\sum_k E_k \cos\left(\frac{\pi k}{N+1}\right)}{N \varepsilon'}, \quad (10)$$

which depends on the initial condition. For the Gibbs state,  $\langle P_k^2 \rangle = k_B T$  leads the numerator of Eq. (2) is equal to zero in the thermodynamical limit.

We here choose three typical initial conditions to verify the above results:

(1) *Initial condition 1*: The initial energy is concentrated on the kinetic energy of the 2 particles in the middle of the chain, i.e.,  $q_n = 0$  and  $p_n = 0$  except  $p_{\frac{N}{2}} = p_{\frac{N}{2}+1} = \sqrt{N \varepsilon'}$ .

(2) *Initial condition 2*: The initial energy is concentrated on the kinetic energy of the 4 particles in the middle of the chain, i.e.,  $q_n = 0$  and  $p_n = 0$  except  $p_{\frac{N}{2}-1} = p_{\frac{N}{2}} = p_{\frac{N}{2}+1} = p_{\frac{N}{2}+2} = \sqrt{N \varepsilon' / 2}$ .

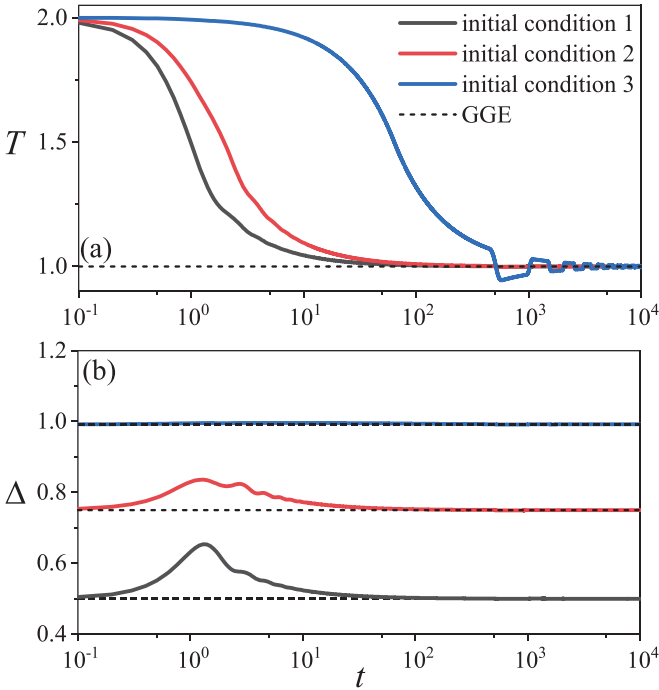


FIG. 1. (a) The temperature  $T$  and (b) the indicator  $\Delta$  as a function of time in semilog scale. The black (lower), red (middle) and blue (upper) solid lines represent initial conditions 1, 2, and 3, respectively. The values predicted by GGE are depicted by dashed black lines. Here,  $\varepsilon' = 1$ .

(3) *Initial condition 3*: The initial energy is concentrated on the kinetic energy of the  $N/8$  particles in the middle of the chain, i.e.,  $q_n = 0$  and  $p_n = 0$  except  $p_{\frac{N}{2}-\frac{N}{16}} = p_{\frac{N}{2}-\frac{N}{16}+1} = \dots = p_{\frac{N}{2}+\frac{N}{16}-1} = \sqrt{8\varepsilon'}$ .

Figure 1(a) depicts the relaxation of the temperature towards a steady-state value  $\varepsilon'$  for different initial conditions, as predicted by GGE. However, as shown in Fig. 1(b), the indicator  $\Delta$  exhibits a dependence on initial conditions, which are in good agreement with Eq. (10).

### B. Quench protocol

In previous studies of thermalization, the initial nonequilibrium state is prepared in the wave-vector space (see, e.g., Ref. [12]). While the indicator  $\Delta$  is defined by the momentum of the real space, one should prepare the nonequilibrium initial condition for real-space thermalization. To ensure that the initial nonequilibrium state is equidistant from the thermal state, the initial value of indicator  $\Delta$  should be the same for different nonintegrable strengths. This motivates us to introduce the quench protocol [33]: An initial (integrable) Hamiltonian  $H(t=0^-)$  is suddenly changed to the new (non-integrable) Hamiltonian  $H(t=0^+)$  by an external operation. This method provides a convenient way to initialize non-integrable systems with a nonequilibrium state originating from an integrable system. While the state of the system  $\Gamma$  remains unchanged at  $t=0^+$ , the energy should be given by the new Hamiltonian  $H(t=0^+)$ . The schematic diagram of the quench protocol is shown in Fig. 2(a).

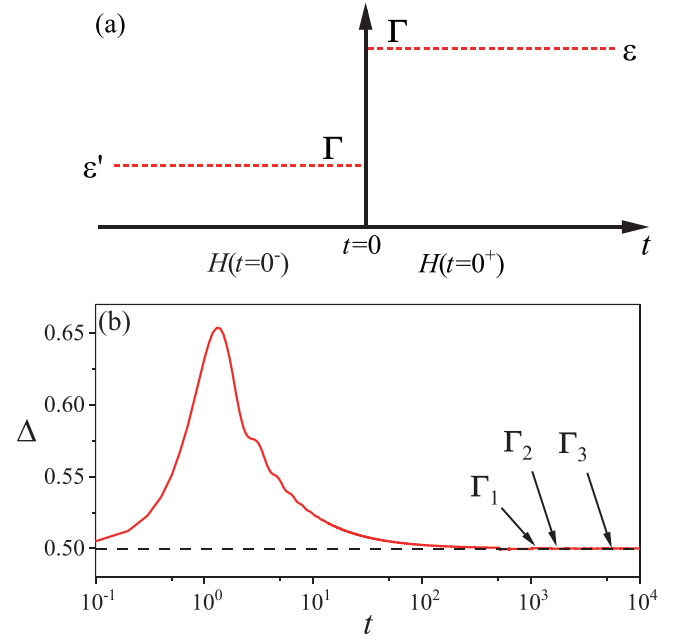


FIG. 2. (a) The schematic diagram of the quench. The state  $\Gamma$  remains unchanged at  $t=0^+$ . However, the energy density is given by the changed Hamiltonian  $H(t=0^+)$ . (b) The indicator  $\Delta$  as the function of time for the initial condition 1. The quench occurs randomly in time after the system relaxes to the GGE state. The observable is averaged different initial states of quench ( $\Gamma_1, \Gamma_2, \Gamma_3, \dots$ ).

To realize the quench protocol, we select the harmonic lattice as the initial integrable system. To reduce the fluctuations of observables, an ensemble average is employed by randomly sampling the quench time, as can be seen in Fig. 2(b). The specific steps of the quench protocol are outlined below:

(1) *Initialization*: The harmonic system is initialized for different initial conditions with energy density  $\varepsilon'$ . Such as initial conditions 1, 2, and 3. Then, the harmonic lattice evolves long enough to reach the GGE state.

(2) *Quench*: After the harmonic system relaxes to the GGE state, the nonintegrable terms are added to the Hamiltonian at a random time  $t_r$  (see Fig. 2). The energy density is changed to  $\varepsilon$  by the new Hamiltonian.

(3) *Thermalization*: The indicator  $\Delta$  as a function of time can be obtained for the relaxation process.

(4) *Average*: Average the energy density  $\varepsilon$  and the indicator  $\Delta(t)$  over the random quench time  $t_r$ .

The SABA<sub>2</sub>C symplectic algorithm [34] is employed to integrate the equations of motion derived from the Hamiltonian Eq. (1), with the fixed boundary condition, i.e.,  $q_0 = 0$  and  $q_{N+1} = 0$ , and the system size  $N = 1024$ . In our simulations, the integration time step is  $\Delta t = 0.01$  and the energy drift is kept less than  $10^{-6}$ . The quench occurs at  $t_r = R \times 10^3$ , where  $R$  is a random variable with the uniform distribution  $R \in U(1, 10)$ . This quench time selection is motivated by the observation that the harmonic system reaches the steady state described by the GGE for  $t > 10^3$  [see Fig. 1(b)]. Here, the energy density  $\varepsilon$  and observables are averaged over 100 realizations for different quench time  $t_r$  to reduce the fluctuations due to the finite-size effect.

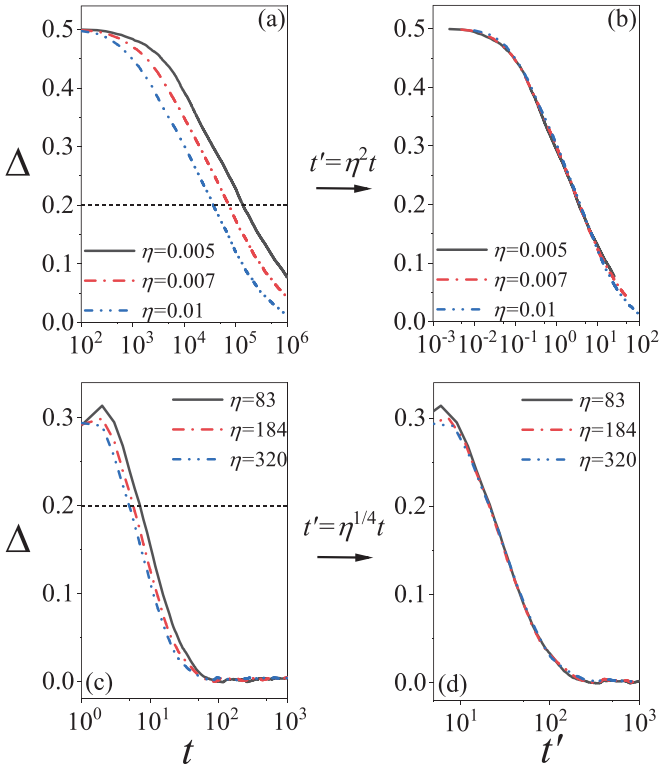


FIG. 3. The indicator  $\Delta$  as a function of time in the semilog scale for (a) the quasi-integrable cases and (c) the strongly nonintegrable cases by different values of  $\eta$ . The horizontal black dashed lines at  $\Delta = 0.2$  are plotted as a threshold for calculating the thermalization time. The indicator  $\Delta$  as the function of rescaling time in semilog scale for (b) the quasi-integrable cases ( $t' = \eta^2 t$ ) and (d) the strongly nonintegrable cases ( $t' = \eta^{1/4} t$ ) by different values of  $\eta$ . The curves collapse to a single one.

### III. RESULTS

We demonstrate the above quench protocol for the FPUT- $\beta$  lattice, which has no onsite potential  $U(x) = 0$  and interaction potential

$$V(x) = \frac{1}{2}x^2 + \frac{\beta}{4}x^4. \quad (11)$$

We rescale the corresponding Hamiltonian (1)  $H' = \varepsilon H$  by  $q'_i = q_i \varepsilon$ , hence the nonlinear parameter  $\beta$  and the energy density have an exact scaling  $\beta' = \beta \varepsilon$ . Therefore, it is equivalent to study the effects of  $\beta$  by fixing  $\varepsilon$  or those of  $\varepsilon$  by fixing  $\beta$ . For convenience, the nonintegrable strength of the FPUT- $\beta$  lattices can be defined as

$$\eta = \beta \varepsilon. \quad (12)$$

In Figs. 3(a) and 3(c), we show the evolution of the indicator  $\Delta(t)$  of initial condition 1 for different values of small and large  $\eta$ , respectively. It is observed that the indicator tends to zero on a sufficiently long timescale, indicating the eventual achievement of thermalization. The thermalization timescale decreases as  $\eta$  increases. In Figs. 3(b) and 3(d), we present the evolution of the indicator  $\Delta$  as the function of the rescaling times  $t' = \eta^2 t$  (for the quasi-integrable case) and  $t' = \eta^{1/4} t$  (for the strongly nonintegrable case) for different

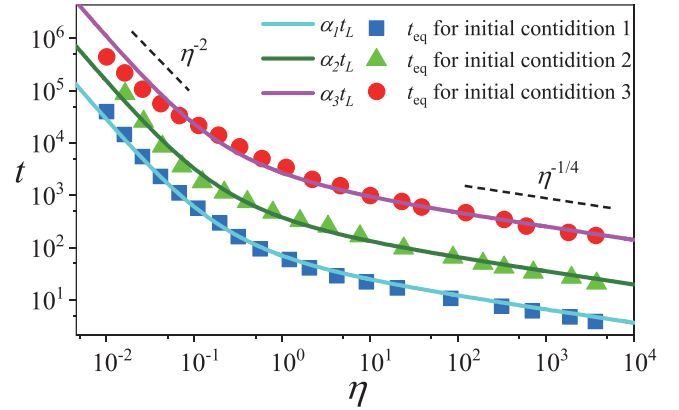


FIG. 4. The thermalization time for different initial conditions. The solid color lines denote  $\alpha t_L$  for different values of proportional coefficients  $\alpha$  to fit the thermalization time for the three different initial conditions. Here,  $\alpha_1 = 13$  (lower cyan line),  $\alpha_2 = 70$  (middle olive line), and  $\alpha_3 = 500$  (upper magenta line). The two dashed lines are drawn for  $t_{\text{eq}} \sim \eta^{-2}$  and  $t_{\text{eq}} \sim \eta^{-1/4}$  as references.

values of  $\eta$ . The curves seem to overlap with each other and collapse to a single one, which implies that the thermalization time shows scaling behaviors  $t_{\text{eq}} \sim \eta^{-2}$  and  $t_{\text{eq}} \sim \eta^{-1/4}$  in the quasi-integrable region and the strongly nonintegrable region, respectively. Note that the Lyapunov time also exhibits the asymptotic behaviors  $t_L \sim \eta^{-1/4}$  as  $\eta \rightarrow \infty$  in FPUT- $\beta$  lattices [35], which suggests a proportionality between the thermalization time and the Lyapunov time in the strongly nonintegrable regime.

The thermalization time can be defined as the time at which the indicator reaches a specific threshold  $\Delta(t_{\text{eq}}) = C$ . While the choice of the threshold  $C$  can change the value of the thermalization time, it does not affect the underlying scaling behavior observed in Fig. 3. For initial conditions 1, 2, and 3, we choose  $C = 0.2, 0.3$ , and  $0.5$  to determine the thermalization time, respectively. The numerical results of the thermalization time of the three initial conditions are presented in Fig. 4. For all three initial conditions, the thermalization time exhibits the same scaling behaviors with power-law exponents of  $-2$  in the quasi-integrable region and  $-1/4$  in the strongly nonintegrable region, which is consistent with the discussion of Fig. 3. Furthermore, in Fig. 4, we also depict the  $\alpha t_L$  as the function of the nonintegrable strength for different  $\alpha$ . The maximum Lyapunov exponent (the inverse of the Lyapunov time) is numerically calculated by the standard method [36]. Figure 5 presents the time evolution of the finite-time Lyapunov exponent estimator  $\lambda$ . This visualization demonstrates that the maximum Lyapunov exponent of the FPUT lattice is independent of the initial conditions. As shown, the finite-time Lyapunov exponents for different initial conditions all reach a constant value after a certain time ( $t > 10^7$ ). Consequently, we adopt the values beyond this saturation point as the system's maximum Lyapunov exponent. As one can see, the thermalization time is approximately proportional to the Lyapunov time

$$t_{\text{eq}} \approx \alpha t_L. \quad (13)$$

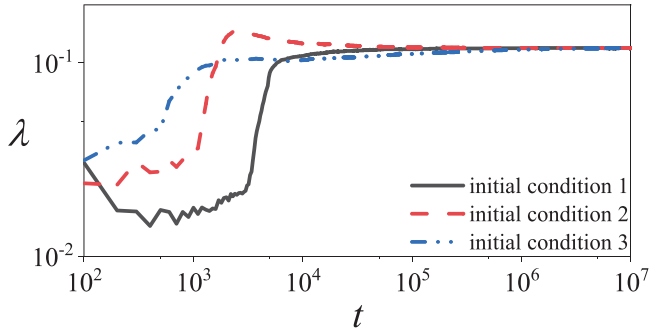


FIG. 5. The finite-time Lyapunov exponent estimator  $\lambda$  as a function of time for three different initial conditions in the log-log scale. Here,  $\eta = 1$ .

where the proportional coefficients  $\alpha$  are different for three initial conditions but independent of the nonintegrable strength. This suggests that the proportional relation holds not only in the quasi-integrable region and the strongly nonintegrable region but over a wide range of the nonintegrable strength, including the intermediate region.

In Fig. 6(a), we present the indicator  $\Delta$  as a function of time for different values of  $\eta$  with the initial condition 3. By rescaling the time as the Lyapunov time  $t' = t/t_L$ , the rescaled curves seem to overlap with each other [Fig. 6(b)], which further confirms that the thermalization time is proportional to the Lyapunov time. In other words, while choosing different thresholds  $C$  changes the value of the thermalization time, it does not affect the underlying scaling behavior nor the proportional relationship with the Lyapunov time. Furthermore, we depict the thermalization time as the function of the nonintegrable strength  $\eta$  for different values of  $C$  in Fig. 6(c). Here, we chose  $C = 0.1$  and  $C = 0.2$  for the initial condition 1 as an example. As one can see, for different values of  $C$ , the thermalization time exhibits the same scaling behavior and the proportional relationship still holds, which agrees with the discussion above.

#### IV. SUMMARY

In summary, we present a scheme to study the thermalization in real space. By investigating the value of  $\Delta$  in the harmonic system, we propose a quench protocol to prepare nonequilibrium initial states suitable for thermalization studies. We then apply this method to the FPUT- $\beta$  lattice. Our results demonstrate that the thermalization time not only exhibits the different scaling behaviors in the quasi-integrable region and the strongly nonintegrable region, respectively, but also has a proportional relation to the Lyapunov time. The consistency of these results across three different initial conditions suggests their general validity for the FPUT- $\beta$  lattice. The calculation of the thermalization time is independent of the wave-vector space, which avoids the risk that the mode energy is ill-defined beyond the quasi-integrable region. Hence, the method can be extended to other models.

Equation (13) paves the way for understanding the relaxation processes and builds a bridge between dynamics

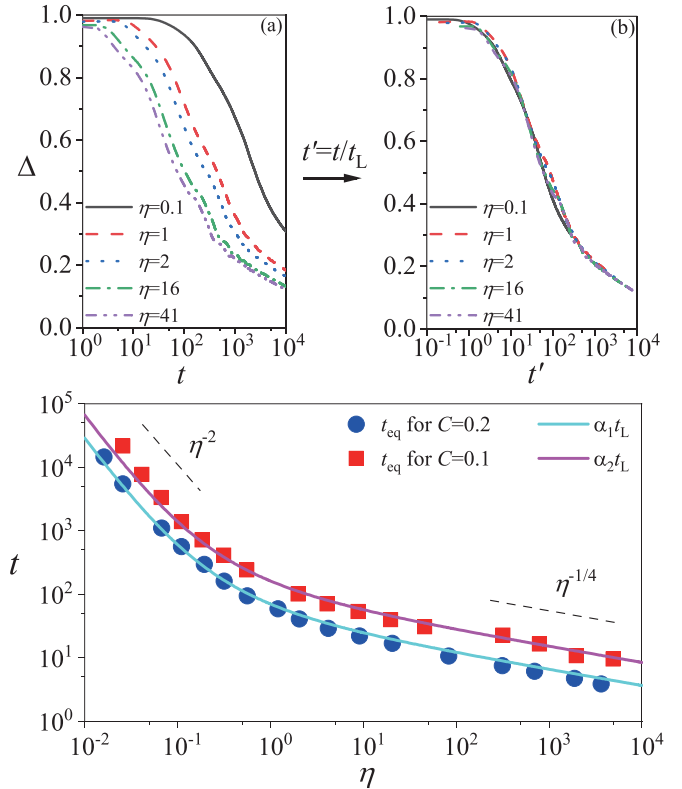


FIG. 6. (a) The indicator  $\Delta$  as the function of time in semilog scale for different values of  $\eta$ . (b) The indicator  $\Delta$  as the function of the rescaling time ( $t' = t/t_L$ ), where the curves overlap with each other. (c) The thermalization time  $t_{\text{eq}}$  for  $C = 0.1$  and  $C = 0.2$ , and  $\alpha t_L$  as a function of the nonintegrable strength  $\eta$  in the log-log scale. The thermalization time exhibits the same scaling behavior for different  $C$ . Moreover, the thermalization time is shown to be proportional to the Lyapunov time within the range of  $\eta$ , and the coefficient of proportionality is  $\alpha_1 = 30$  for  $C = 0.1$  (upper cyan line) and  $\alpha_2 = 13$  for  $C = 0.2$  (lower magenta line).

and statistical mechanics. Instead of an absolute time, the thermalization time is a characteristic time, which captures the average rate of thermalization. While alternative observables could potentially serve as indicators for defining characteristic thermalization times, these timescales should exhibit qualitatively similar behaviors, including the observed scaling laws and, potentially, the proportionality to the Lyapunov time, a quantity that intrinsically characterizes chaotic systems. The applicability of our proposed scheme extends beyond the FPUT- $\beta$  lattice. Further investigation is warranted to verify the validity of Eq. (13) in a broad range of Hamiltonian systems. The observed proportionality relationship in the FPUT- $\beta$  lattice could be an approximation of a more rigorous formula, which merits dedicated research efforts.

The Toda lattice, a well-known nonlinear integrable model [37,38], can also be described by GGE, whose indicator  $\Delta$  approach to nonzero values depends on initial conditions. The equilibration process observed in the Toda lattice [23] might correspond to the system relaxing towards the GGE steady state. The Toda lattice has been extensively

studied for comparison to the short-time dynamics of the FPUT lattice [12,13]. By comparing the values of  $\Delta$  in Toda lattices with the values in the metastable state of FPUT lattice for small  $\eta$  to gain further insights into how the Toda lattice serves as the integrable limit of the FPUT model. Instead of the harmonic lattice, the Toda lattice, even the monatomic gas model, which can provide a good enough nonequilibrium initial state after quenching for different system parameters, can also be used as the quenched model.

## ACKNOWLEDGMENTS

The authors acknowledge helpful discussions with Hong Zhao, Jiao Wang, Yong Zhang, and Zhen Wang. This work was financially supported from the National Natural Science Foundation of China (Grants No. 12075199 and No. 12247172), the Natural Science Foundation of Fujian Province (Grant No. 2021J01006), and the Natural Science Foundation of Jiangxi Province (Grant No. 20212BAB201024). Numerical simulations were performed on TianHe-1 (A) at National Supercomputer Center in Tianjin.

- 
- [1] G. Gallavotti, *The Fermi-Pasta-Ulam Problem: A Status Report* (Springer, New York, NY, 2008)
- [2] M. Onorato, L. Vozella, D. Proment, and Y. V. Lvov, *Proc. Natl. Acad. Sci. USA* **112**, 4208 (2015).
- [3] A. M. Kaufman, M. E. Tai, A. Lukin, M. Rispoli, R. Schittko, P. M. Preiss, and M. Greiner, *Science* **353**, 794 (2016).
- [4] C. Gogolin and J. Eisert, *Rep. Prog. Phys.* **79**, 056001 (2016).
- [5] L. P. García-Pintos, N. Linden, A. S. L. Malabarba, A. J. Short, and A. Winter, *Phys. Rev. X* **7**, 031027 (2017).
- [6] K. Mallayya, M. Rigol, and W. De Roeck, *Phys. Rev. X* **9**, 021027 (2019).
- [7] Z. Wang, W. Fu, Y. Zhang, and H. Zhao, *Phys. Rev. Lett.* **124**, 186401 (2020).
- [8] E. Fermi, J. Pasta, and S. Ulam, in *Collected Papers of Enrico Fermi*, edited by E. Segré (University of Chicago Press, Chicago, IL, 1965), Vol. 2, p. 978.
- [9] N. J. Zabusky and M. D. Kruskal, *Phys. Rev. Lett.* **15**, 240 (1965).
- [10] J. P. Eckmann and D. Ruelle, *Rev. Mod. Phys.* **57**, 617 (1985).
- [11] E. Fucito, F. Marchesoni, E. Marinari, G. Parisi, L. Peliti, S. Ruffo, and A. Vulpiani, *J. Phys. France* **43**, 707 (1982).
- [12] G. Benettin and A. Ponno, *J. Stat. Phys.* **144**, 793 (2011).
- [13] A. Ponno, H. Christodoulidi, C. Skokos, and S. Flach, *Chaos* **21**, 043127 (2011).
- [14] G. Benettin, H. Christodoulidi, and A. Ponno, *J. Stat. Phys.* **152**, 195 (2013).
- [15] W. Fu, Y. Zhang, and H. Zhao, *New J. Phys.* **21**, 043009 (2019).
- [16] W. Fu, Y. Zhang, and H. Zhao, *Phys. Rev. E* **100**, 010101(R) (2019).
- [17] W. Fu, Y. Zhang, and H. Zhao, *Phys. Rev. E* **100**, 052102 (2019).
- [18] L. Pistone, S. Chibbaro, M. Bustamante, Y. Lvov, and M. Onorato, *Math. Biosci. Eng.* **1**, 672 (2019).
- [19] Y. Liu and D. He, *Phys. Rev. E* **103**, L040203 (2021).
- [20] G. Parisi, *Europhys. Lett.* **40**, 357 (1997).
- [21] T. Mithun, C. Danieli, Y. Kati, and S. Flach, *Phys. Rev. Lett.* **122**, 054102 (2019).
- [22] C. Danieli, T. Mithun, Y. Kati, D. K. Campbell, and S. Flach, *Phys. Rev. E* **100**, 032217 (2019).
- [23] S. Ganapa, A. Apte, and A. Dhar, *J. Stat. Phys.* **180**, 1010 (2020).
- [24] In the origin paper [20], this indicator was written as  $\Delta = \langle \sum_n q_n q_{n+1} \rangle / \langle \sum_n q_n^2 \rangle$ , which does not tend to zero in the thermal state in general. While the indicator Eq. (2) generally tends to zero for general case.
- [25] M. Rigol, A. Muramatsu, and M. Olshanii, *Phys. Rev. A* **74**, 053616 (2006).
- [26] M. Rigol, V. Dunjko, V. Yurovsky, and M. Olshanii, *Phys. Rev. Lett.* **98**, 050405 (2007).
- [27] L. Vidmar and M. Rigol, *J. Stat. Mech.* (2016) 064007.
- [28] P. Calabrese, F. H. L. Essler, and M. Fagotti, *Phys. Rev. Lett.* **106**, 227203 (2011).
- [29] F. H. L. Essler, S. Evangelisti, and M. Fagotti, *Phys. Rev. Lett.* **109**, 247206 (2012).
- [30] T. M. Wright, M. Rigol, M. J. Davis, and K. V. Kheruntsyan, *Phys. Rev. Lett.* **113**, 050601 (2014).
- [31] G. Mussardo, *Phys. Rev. Lett.* **111**, 100401 (2013).
- [32] E. Ilievski, J. De Nardis, B. Wouters, J.-S. Caux, F. H. L. Essler, and T. Prosen, *Phys. Rev. Lett.* **115**, 157201 (2015).
- [33] F. H. L. Essler and M. Fagotti, *J. Stat. Mech.* (2016) 064002.
- [34] C. Skokos and E. Gerlach, *Phys. Rev. E* **82**, 036704 (2010).
- [35] L. Casetti, R. Livi, and M. Pettini, *Phys. Rev. Lett.* **74**, 375 (1995).
- [36] G. Benettin, L. Galgani, and J.-M. Strelcyn, *Phys. Rev. A* **14**, 2338 (1976).
- [37] M. Toda, *Phys. Rep.* **18**, 1 (1975).
- [38] M. Toda, *Phys. Scr.* **20**, 424 (1979).